# Max-Planck-Institut
## für Mathematik
## in den Naturwissenschaften
## Leipzig

STDP-driven networks and the *C. elegans* neuronal network

by

*Quansheng Ren, Kiran M. Kolwankar, Areejit Samal, and Jürgen Jost*

# STDP-driven networks and the *C. elegans* neuronal network

Quansheng Ren,[1] Kiran M. Kolwankar,[1,2] Areejit Samal,[1,3] and Jürgen Jost[1,4]

[1]*Max Planck Institute for Mathematics in the Sciences, Inselstr. 22, D-04103 Leipzig, Germany*
[2]*Department of Physics, Ramniranjan Jhunjhunwala College, Ghatkopar (W), Mumbai 400 086, India*
[3]*Laboratoire de Physique Théorique et Modèles Statistiques,*
*CNRS and Univ Paris-Sud, UMR 8626, F-91405 Orsay, France*
[4]*The Santa Fe Institute, 1399 Hyde Park Road, Santa Fe, New Mexico 87501, USA*[*]

We study the dynamics of the structure of a formal neural network wherein the strengths of the synapses are governed by spike-timing-dependent plasticity (STDP). For properly chosen input signals, there exists a steady state with a residual network. We compare the motif profile of such a network with that of a real neural network of *C. elegans* and identify robust qualitative similarities. In particular, our extensive numerical simulations show that this STDP-driven resulting network is robust under variations of the model parameters.

## INTRODUCTION

In any theoretical study on neuronal networks, the formal structure of the network as a directed graph is an important ingredient which, in reality, can be rather complicated. In the last decade, statistical concepts and tools have been developed for analyzing the large scale properties of complex networks [1–5]. On this theoretical basis, it has been found that neural networks can exhibit scale free and small world properties [6, 7]. For a more refined analysis and the identification of deeper properties that may or may not distinguish neuronal networks from other classes of biological or non-biological networks, it is necessary to identify those factors that determine the structure of neuronal networks. Naively, one might think that the structure of a neuronal network is determined genetically. But for animals with larger brains, this would require an enormous amount of genetically encoded information. In other words, at best the connections of a few important axons could be genetically encoded. Moreover, several experimental findings we decribe below suggest a lack of any hard-wired programme of axon guidance. Another possible factor could be geometric constraint since the network is embedded in a small three dimensional volume. This is likely to affect only the long range connections and not the local structure, and in any case, this constraint seems to be too unspecific. Therefore, we should expect that some self-organization process yields the connectivity structure of neuronal networks. As most biological self-organization processes are triggered by external factors or signals, we should also look here for sources of external influences. Since a neuronal network processes sensory inputs, it should thereby adapt itself to its experiences. Hence, we are naturally led to consider learning as a key factor guiding the self-organization of a neuronal network. The standard Hebbian paradigm tells us that learning is represented by modifications of the strengths of the synapses between neurons. In particular, learning is local in the sense that it depends on correlations between the activities of synaptically connected neurons. In more biological detail, we have the learning scheme of *spike timing dependent synaptic plasticity* first discovered in [8], abbreviated as STDP. This learning rule says that a synapse is strengthened when the presynaptic neuron fires shortly before the postsynaptic one, and that it is weakened instead when this temporal order is reversed. This learning rule has received a lot of attention in the neurobiological literature. In [9], it has been formally analyzed how this learning rule, being based on activity correlations, in turn shapes these correlations. Again, this is a local rule, but it is then natural to expect that the global statistical properties of neuronal networks result from the iterated application of this local rule at all the active synapses of the network. In particular, some synapses could possibly become so weak that they will get eliminated entirely.

The initial explorations to test this line of thinking have been encouraging [10, 11]. In [10], in order to separate the abstract features of this learning rule from the details of its neurobiological implementation, we have considered a simple model of coupled chaotic maps wherein the coupling stengths changed according to this learning rule. Starting from a globally coupled network, we obtained a stationary network with a broad degree distribution in accordance with the experimental findings for real neural networks. In [11], similar conclusions were arrived at using a continuous Fitzugh-Nagumo model.

These developments suggest that the learning dynamics may be a relevant factor in determining the network structure. A closer comparison is needed to confirm this conjecture. To this effect we carry out simulations with realistic models of neural dynamics and compare the resultant network with a real one, that is, the neuronal network of *C. elegans*. The neuronal network of *C. elegans* has been studied in detail [12, 13]. In fact, this is the only real neuronal network where such detail is currently available, and, unfortunately, we therefore are not able to use other

experimentally determined networks for comparison. In any case, in learning, there are various kinds of plasticities and different kinds of connections, like, chemical synapses, gap junctions etc. Here we work with realistic neuron models, the STDP learning rule and properly chosen input signals. We show that applying this scheme formally leads to a network which is similar to the network in *C. elegans* in certain aspects.

It is known that the brain has a very dense population of synaptic connection just after the birth and most of these connections are pruned in the course of time [14]. This type of pruning takes place even in *C. elegans* where the size of the network is very small [15]. It has also been shown that the perturbed sensory activity or the mutations that alter the calcium channels or membrane potential affect the axon outgrowth [16]. This is reflected by the irreversible deletion of synapses whose strength falls below a certain threshold.

The plan of the paper is as follows. In section , we decribe the neuron models used, the STDP learning rule and also the tools used to analyse the network. The present status of our knowledge of *C. elegans* network is recalled in section . This section also includes a more detailed analysis of *C. elegans'* neuronal network. The main results of the paper are presented in section ; in particular, we describe the influence of the input and of different parameters on the final results. The paper ends with a discussion in section .

## METHODS

### Neuron models

Networks of neurons were modeled using the NEST Simulation Tool [17]. To show the generality of the results, two models for neurons are utilized, i.e. the Leaky Integrate-and-Fire (LIF) model and the Hodgkin-Huxley (HH) model.

The membrane potential $V_j$ of the conductance based LIF neuron with index $j$ is governed by

$$C_m \frac{dV_j}{dt} = g_L(V_{rest} - V_j) + g_j(t)(E_{ex} - V_j) , \qquad (1)$$

where $C_m = 200$pF is the membrane capacitance, $g_L = 10$nS is the leak conductance which is equivalent to $R_m = 100$MΩ where $R_m$ is the membrane resistance, $V_{rest} = -70$mV is the resting potential (leak reversal potential), $E_{ex} = 0$mV is the excitatory reversal potential. In our simulation, we did not consider inhibitory synapses as they are extremely rare between interneurons in the *C. elegans* neuronal network (see Section ). When the membrane potential reaches the threshold value $V_{th} = -54$mV, the neuron emits an action potential, and the depolarization is reset to the reset potential $V_{reset} = -60$mV after a refractory period $\tau_{ref} = 1$ms during which the potential is insensitive to stimulation. The parameters given above are the same as in [18].

The dynamical equation for the Traub modified conductance based Hodgkin-Huxley model neuron is

$$C_m \frac{dV_j}{dt} = g_L(E_L - V_j) + g_{Na}m^3h(E_{Na} - V_j) + g_K n^4(E_K - V_j) + g_j(t)(E_{ex} - V_j), \qquad (2)$$

where $C_m = 100$pF. $E_{ex} = 0$mV is the excitatory reversal potential. The maximal conductances and reversal potentials of the sodium and potassium ion channels and the leak channel used in the model are $g_{Na} = 1.0$mS/mm$^2$, $g_K = 2.0$mS/mm$^2$, $g_L = 0.001$mS/mm$^2$, $E_{Na} = 48$mV, $E_K = -82$mV, and $E_L = -67$mV respectively. The gating variables $X = m, h, n$ satisfy the following equation:

$$\frac{dX}{dt} = \alpha_X(V_j)(1 - X) - \beta_X(V_j)X, \qquad (3)$$

where $\alpha_X$ and $\beta_X$ are given by

$$\alpha_m = \frac{0.32(V + 54)}{1 - \exp(-0.25(V + 54))} \quad \beta_m = \frac{0.28(V + 27)}{\exp(0.2(V + 27)) - 1}$$

$$\alpha_h = 0.128\exp(-(V + 50)/18) \quad \beta_h = \frac{4}{1 + \exp(-0.2(V + 27))}$$

$$\alpha_n = \frac{0.032(V + 52)}{1 - \exp(-0.2(V + 52))} \quad \beta_n = 0.5\exp(-(V + 57)/40).$$

These parameters are taken from [19].

The synaptic conductance $g_j(t)$ in Eq. (1) and (2) is determined by

$$g_j(t) = g_m \sum_{j=1}^{N} w_{ij}(t) \sum_k f(t - t_j^k) , \qquad (4)$$

where N is the number of neurons, $g_m$ is the maximum value of the synaptic conductance, $w_{ij}$ is the weight of the synaptic connection from the $i$th neuron to the $j$th neuron, $t_j^k$ is the timing of the $k$th spike of the $j$th neuron. Here, we used an $\alpha$-function [20] $f(x)$ with latency (transmission delay) $\tau_d$ and synaptic time constant $\tau_{ex} = 2$ms:

$$f(t) = \begin{cases} \frac{t - \tau_d}{\tau_{ex}^2} \exp(-\frac{t - \tau_d}{\tau_{ex}}) & \text{if } t > \tau_d \\ 0 & \text{otherwise.} \end{cases} \qquad (5)$$

## STDP

STDP is a form of experimentally observed ([8]) long-term synaptic plasticity, where synapses are modified by repeated pairings of pre- and postsynaptic action potentials, while the sign and the degree of the modification depend on their relative timing.

In our study, the weight of the synaptic connection $w_{ij}$ is modified by the STDP rule. The amount of modification is determined based on the temporal difference $\Delta t$ between the occurrence of the postsynaptic action potential and the arrival of the presynaptic action potential,

$$\Delta t = t_j - (t_i + \tau_d), \qquad (6)$$

where $t_j$ is the spike time of the postsynaptic neuron $j$, $\tau_d$ is the delay time of the spike transmission from neuron $i$ to neuron $j$, and $t_i$ is the spike time of the presynaptic neuron $i$. The weight modification $\Delta w_{ij}$ is described by the following equations:

$$\Delta w_{ij}(\Delta t) = \begin{cases} \lambda \exp(-|\Delta t|/\tau_+) & \text{if } \Delta t \geq \tau_d \\ -\lambda \alpha \exp(-|\Delta t|/\tau_-) & \text{if } \Delta t < \tau_d, \end{cases} \qquad (7)$$

where $\lambda = 0.0001$ is the learning rate. We constrain $w_{ij}$ within the range $[0,1]$, which ensures that the peak synaptic conductance $g_m w_{ij}$ is always positive and cannot exceed the maximum value $g_m$. In Eq. 7, $\alpha$ introduces a possible asymmetry between the scale of potentiation and depression. The time constants $\tau_+$ and $\tau_-$ control the width of the time window. As argued in [18], in order to get a stable competitive synaptic modification, which means that uncorrelated pre- and postsynaptic spikes produce an overall weakening of synapses, the integral of $\Delta w_{ij}$ should be negative. A negative integral requires $(\alpha \tau_- / \tau_+) > 1.0$.

## Network Motifs

To test whether STDP plays a crucial role in the evolution of a real neuronal network, it is important to compare the local structure between real networks and the network we obtain as a result of our simulations. We choose to look at the occurrence of different network motifs. Network motifs are patterns (sub-graphs) that recur within the network much more often than expected at random [21]. The characterisation of networks using network motifs has become very common owing to the fact that different subnetworks are thought to carry out different functions in the network and the abundance of certain subnetworks can decide the overall character of the network. In order to determine the relative occurrence of motifs one needs to generate random versions of the network and count the number of motifs. The question of the choice of the null model and the method used to generate random networks is important. We use the approach and the software mfinder developed by Alon and co-workers [21, 22]. First, numbers of different three-node subgraphs in a given network are found. Then, we compare the network to an ensemble of randomized networks, whose number is 1000 in this study. Randomization is performed by rewiring connections in such a way that the number of incoming edges, outgoing edges and mutual edges of each node are preserved. For each subgraph $i$, the statistical significance is defined by its Z-score:

$$z_i = \frac{N_i^{real} - \langle N_i^{rand} \rangle}{std(N_i^{rand})}, \qquad (8)$$

where $N_i^{real}$ is the frequency of subgraph $i$ appearing in the real network, $\langle N_i^{rand} \rangle$ and $std(N_i^{rand})$ are the mean and standard deviation of subgraph $i$'s occurrences in the ensemble of random networks. If $z_i > 0$, subgraph $i$ is over-represented and is designated as a motif, while if $z_i < 0$, it is under-represented and is designated as a anti-motif. The significance profile (SP) of a network is the vector of Z-scores normalized to length 1:

$$SP_i = \frac{z_i}{\sqrt{\sum_i^{13} z_i^2}}. \tag{9}$$

It shows the relative significance of subgraphs and is important for comparison of networks of different sizes and degree sequences. The software mfinder [23] has integrated all the above algorithms.

To construct random ensembles, one often uses Occam's razor, i.e. no outcome compatible with the null hypothesis should be preferred and all such outcomes are equally likely [24]. The approach mentioned above uses the random ensemble with fixed degree sequence and fixed number of 2-node subgraphs for each node as the relevant null model. We should point out here that a more conceptual approach [25, 26] leads to somewhat different null hypotheses, as will be briefly discussed in Section . In particular, the SPs of different motifs are not independent. That is, a change in some motif can also affect the count of another motif and hence its SP. In spite of these and many other complications, Milo et al. [22] have discovered four superfamilies with distinct motif diagrams. The second superfamily included signal-transduction networks, developmental transcription networks of multi-cellular organisms and the *C. elegans* neuronal network. The existence of such "universality classes" of different natural as well as artificial networks makes this approach of characterising complex networks, which are otherwise rather untractable, very promising. Several explanations [22, 27, 28] have been proposed to explain the observed convergence of SPs of these networks. In particular, robustness against node or link failure has been invoked a global optimization criterion leading to such particular motif distributions as in the superfamilies. Our study provides an alternative explanation in terms of a local self-organization rule, i.e. the common SP of the second superfamily may come from an adaptive mechanism in cooperation with the complex structure of correlations between input signals.

## C. ELEGANS NEURONAL NETWORK

In this section we discuss the neuronal network of *C. elegans*. It is a small sensory transduction neuronal network that consists of sensory neurons, interneurons and motor neurons. In this study, the most recently published wiring diagram of *C. elegans* [13] is used. The somatic neuronal network contains 279 neurons which are connected by 2194 directed connections implemented by one or more chemical synapses, and 514 gap junction connections consisting of one or more electrical junctions. We point out that, in contrast to vertebrates, there are no individual variations among different members of the species *C. elegans* here. As STDP can only operate in chemical synapses, we restrict our attention to the chemical synapse network. However, one should note that the bidirectional gap connections could influence the dynamics of neurons, which, in turn, could influence the network topology further by plasticity mechanisms like STDP.

From fig. 1, we see that the connections both from sensory neurons to interneurons or from interneurons to motor neurons are more numerous than the connections from interneurons to sensory neurons or from motor neurons to interneurons respectively. On the other hand, there are rare connections between sensory neurons and motor neurons. External signals first arrive at sensory neurons, then propagate through some interneurons and finally reach a subset of motor neurons to generate a stimulus-induced response. Both sensory neurons and motor neurons have preferred connections to neighboring neurons and can be divided into several clusters, which may correspond to different functions. However, the pool of interneurons is not organized into clusters or layers. Each signal passes through a few interneurons before it reaches motor neurons. We want to study the network structure generated by the STDP-driven pruning process from a pool of homogeneous neurons. From this point of view, the pool of interneurons in *C. elegans* is more related to our case than sensory neurons and motor neurons. There are 82 interneurons and 479 connections between them, among which there are 122 mutual links and 357 uni-directional links. Moreover, there is only 1 inhibitory synapse between interneurons according to the latest data and a rough approximation that GABAergic synapses are inhibitory [13]. Fig. 2 shows the triad subgraph frequency spectrum of the subnetwork of interneurons and the whole neuronal network in *C. elegans*.

The SP of the *C. elegans* neuronal network has previously been shown in [22]. Some motif analysis of the latest wiring diagram has also been presented in [13]. However, the local structure may be quite different for different functional networks. Here we calculate SPs for different categories of neurons in *C. elegans* separately. Fig. 4 shows the SPs of different subnetworks with only sensor neurons, only motor neurons, only interneurons, the combination

of sensor neurons and interneurons, the combination of motor neurons and interneurons, and the whole neuronal network respectively. Comparing these SPs, we found that the SP characteristic of *C. elegans* neural system reported previously [13, 22] mainly comes from the connectivity structure of interneurons. The SP of interneurons subnetwork shows triads 7, 9 and 10 as motifs, triads 1, 2, 4, 5 and 6 as anti-motifs, and there is less bias against cascades (triad 3). In this paper we focus on the question whether these observed motifs could be generated via self-organization through STDP.

## EVOLUTION OF NEURAL NETWORKS WITH STDP

It is known that the density of synapses in the human frontal cortex continues to increase during infancy and remains at a very dense level. After a short stable period, synapses begin to be constantly removed, yielding a decrease in synaptic density. This pruning process continues until puberty, when synaptic density achieves adult levels [29]. As such a pruning of synapses that are in some sense superfluous may be a rather universal process, we study the local structure of a network obtained by an STDP-driven pruning process, and compare it with *C. elegans*.

### Basic phenomena

To simulate the STDP-driven pruning process, we start the simulations with an all-to-all connected network. The neurons are stimulated by different periodic patterns repeatedly with period $T_{pattern}$. All the patterns are truncated from Poisson spike trains with the same average rate $f_{Poisson} = 50$Hz. This average firing rate corresponds to a 20ms spike interval which is consistent with the width of STDP time window. The connections between neurons are excitatory STDP synapses. Because GABAergic synapses are extremely rare between interneurons of *C. elegans*, we do not consider inhibitory synapses here.

Because of the asymmetry between the scale of potentiation and depression, most synapses are weakened during the learning process. The peak synaptic conductances approach a bimodal distribution. Then we filter the adjacency matrix by a small threshold: If the weight of a synapse is less than the threshold, we consider it as a pruned synapse, i.e. there is no connections, otherwise we consider it as a winning synapse. At last, an unweighted adjacency matrix is obtained. We analyze the local structure of the network, and compare it with *C. elegans*. To simulate the long term development of neural systems, we used a small learning rate ($\lambda = 0.0001$) and simulated for more than $10^7$ms. All the peak synaptic conductances and the potentials of neurons are initialized with a random uniform distribution. After development, most of the peak synaptic conductances are pushed toward zero or $g_m$ (cf. fig. 5a). We set the threshold to $g = 0.005$nS, under which the synapses are seen as pruned. Fig. 5b shows the variation in the number of links, i.e. the number of the synapses whose peak conductance is above the threshold. We see that the number of links decreases rapidly before $10^6 ms$, and toward the end the distribution of peak synaptic conductances remains almost constant except for tiny fluctuations, i.e. a steady-state condition is achieved. We then analyze the occurrence of triad motifs in the resulting steady-state network.

Following the preceding approach, we study four cases with different configurations. The first case is called the "basic configuration", and later cases are variations of this one. For this "basic configuration", we simulate a small network with $N = 100$ LIF neurons, which is of a similar size as the subnetwork of somatic interneurons in *C. elegans*. We used an asymmetric time window $\tau_+ = 16.8$ms and $\tau_- = 33.7$ms in STDP rule, which provides a reasonable approximation of the synaptic modification observed in actual experiments [30]. $\alpha = 0.525$ is adopted, together with the asymmetric time window, providing a ratio $A_-\tau_-/A_+\tau_+ = 1.05$ which is the same as in [18]. Other parameters are set as follows: the synaptic delay $\tau_d = 10$ms, the maximum peak synaptic conductance $g_m = 0.3$nS, and the period of input patterns $T_{pattern} = 2$s. Based on the "basic configuration", we study three variations: "Symmetric configuration", where the asymmetric time window is replaced with a symmetric one ($\tau_+ = \tau_- = 20.0$ms), and $\alpha = 1.05$ to preserve the ratio $A_-\tau_-/A_+\tau_+ = 1.05$; "HH model configuration", where LIF model is replaced by the HH model; "Large network configuration", where the network size is enlarged to 200 neurons, and $g_m = 0.2$nS in this case. For every configuration, we simulate 10 times with different input patterns, different initial potential of neurons and different initial peak synaptic conductances. We calculate the SP of every simulation and compute the average of 10 SPs.

Fig. 6 shows the SPs of the four configurations and compares them with the *C. elegans* neuronal network. All the four STDP-driven evolved network have quite similar SPs. All of them show triads 7, 9, and 10 as motifs, and triads 1, 2, 4, 5, as anti-motifs, as in the *C. elegans* neuronal network which belongs to the second superfamily reported in [22]. This phenomenon does not depend on the neuron model, the symmetry of the time window or the network

size, and so must reflect some intrinsic characteristic of STDP. Recently, several interesting functions and dynamics have been found to be associated with the three motifs mentioned above [31]. For example, the feedforward loop (FFL, triad 7) has been shown to perform signal-processing tasks such as acceleration and delay of response, and the mixed-feedforward-feedback loops (MFFL1: triad 9, and MFFL2: triad 10), where two-node feedbacks that regulate or are regulated by a third node, have been shown to perform long- and short-term memory. These functions are important for almost all neural computation and cognition tasks, which may give an explanation for the redundance of these motifs in the *C. elegans* neuronal network. Our results show that STDP may be a potential mechanism which could develop these important motifs.

The SP curves of STDP-driven evolved networks are quite similar to the *C. elegans* neuronal network, especially the subnetwork of interneurons, but not the subnetwork of sensor neurons or moter neurons (see fig. 4). This could mean that though STDP determines the structure of the network of interneurons, possibly other factors are important in the case of sensory neurons. Nevertheless, there are small differences between our evolved networks and the subnetwork of interneurons in *C. elegans*. As the SP is the vector of Z-scores normalized to length 1, here we only need to consider the relative relations between triads as well as the zero axis. In STDP-driven evolved networks, triads 1, 2 and 8 have relatively lower negative SP, while triads 3 and 7 have relatively higher positive SP than the ones in the *C. elegans* neuronal network. STDP tends to form feedforward structures [32, 33] and reflect the causal relations between neurons, which could lead to more representations of cascades (triad 3) and FFL (triad 7), and less representations of cycles (triad 8). On the other hand, there are hundreds of gap connections and other properties in the *C. elegans* neuronal network, which we neglect here. The gap connections could certainly influence the dynamics of neurons, while the latter would influence the network structure if there is a certain plasticity mechanism like STDP.

To study the similarity further, we calculated the triad frequency spectra of STDP-driven evolved networks and compare them with the one of the *C. elegans* network. From fig. 7 we see that the STDP-driven evolved network of the "basic configuration" develops a similar triad frequency spectra as that of *C. elegans*.

**The role of neuronal inputs.**

It appears that the inputs received by a neuron play an important role in determining the final network structure. This is already borne out in the experiments [16]. We investigate this point in our simulations. Besides periodic patterns obtained from Poisson spike trains, we also stimulate neurons with other spike trains, such as stochastic Poisson spike trains and periodic regular patterns. In these cases, we either do not obtain a steady distribution of peak synaptic conductances or else find a similar SP. We identify a factor that is crucial for the similarities of the local structure between STDP-driven evolved networks and the *C. elegans* neuronal network: The complexity of correlations between neuronal inputs.

There seem to be two ways to achieve a constant distribution of peak synaptic conductances through STDP: One is to use constant temporal correlations between inputs. The other is through the repeated input of the same temporal sequences [34]. To investigate the former case, we utilize a simple method to generate sufficiently complex temporally correlated inputs: A non-periodic Poisson spike train, whose average firing rate is 50Hz, is randomly delayed for 100 times to generate the inputs of 100 neurons. The random delay time $T_d$ follows a uniform distribution between [1ms, T]. We study two cases: T=20ms and T=200ms. Considering the width of time window in STDP and average spike interval (both ≈20ms), the case of T=20ms corresponds to a high degree and a simple relation structure of temporal correlations between neuronal inputs, while the case of T=200ms corresponds to a more complex relation structure. From fig. 8a we see that the case of T=200ms generates an SP quite similar to that of the interneurons in *C. elegans*, and the only evident difference is in Triad 12. However, in the case of T=20ms we do not obtain such a result. This not only confirms that STDP may play a fundamental role in the formation of the local structure of neuronal networks, but also prompts us to pay attention to the complexity of correlations between neuronal inputs.

On the other hand, this simple scheme of temporally correlated inputs did not generate a triad frequency spectrum similar to that of *C. elegans* (fig. 8b and c). In the case of T=200ms, it generates more triads belonging to a feedforward structure, i.e. cascades (triad 3), FFL (triad 7) and MFFL (triad 9 and 10), but could not generate any subgraph of triads 6, 8 and 11. This may be because the correlation scheme we utilize here is not complex enough as compared to real cases. In *C. elegans*, because of the stochastic characteristic in the environment, common stimuli among adjacent sensory neurons and the sensory network structure, inputs of interneurons could have very complex temporal correlations. It seems difficult to simulate the same temporal correlated neuronal inputs as in *C. elegans*.

However, the repeating of temporal sequences plays an alternative role in generating complicated correlated neuronal inputs. The finite size of sequences brings out non-trival temporal correlations, which could be acumulated by repeating input. The complexity of the non-trival correlations is determined by the input sequences. Partial information of
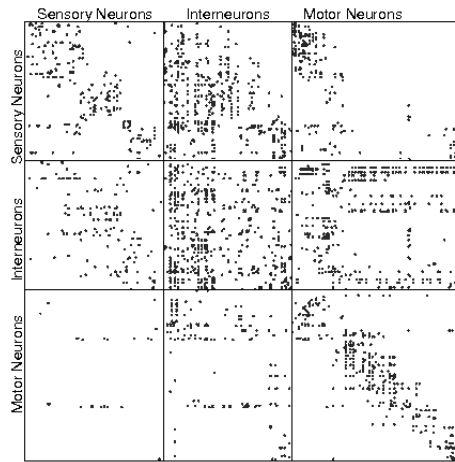
FIG. 1: Adjacency matrix of the chemical synapse network with neurons grouped by category (sensory neurons, interneurons, and motor neurons). Within each category, neurons are in anteroposterior order. The figure is reconstructed from the data contained in [13].

sequences is transformed into a network of stronger or weaker synapses among the neurons. The evolved local network structure reflects certain intrinsic characteristic of input sequences. The temporal sequences we used is truncated from a Poisson process, which provides an extremely useful approximation of stochastic neuronal firing. It could provide enough complexity in the structure of correlations between inputs, which gives rise to a similar triad frequency spectrum as that of *C. elegans* (fig. 7). Otherwise, if regular sequences or simply correlated inputs are used, we do not get similar results.

As the characteristic of correlations comes from a finite-size effect and the characteristic of input sequences, it should not depend on other factors, such as the period of repeating. To verify this, we study two more cases: the effect of input spikes period (the length of repeated spike sequence), and mixing with non-periodic stochastic spikes.

Fig. 9 shows the effect of input spikes period on SPs of networks with different asymmetric parameter $\alpha$ of STDP. We see that the SP does not change when different periods in the range from 150ms to 9s are used confirming that the particular SP we found does not depend on the details of the spike sequence, but the statistical characteristic of a Poisson process. Fig. 10 shows the number of surviving links in networks with input consisting of spike trains of different periods. For longer periods, the stochastic aspects of the spike trains play the leading role, and it is more difficult for synapses to survive under the condition $\alpha\tau_-/\tau_+ > 1.0$. On the other hand, for smaller periods, the finite-size effects of the spike trains play the leading role, and it is easier for synapses to survive. The neuronal network of *C. elegans* is a very sparse network. By using a large period, we could also achieve a sparse network that has a similar number of links as in *C. elegans*, e.g. when $T_{pattern} = 9$s and $\alpha = 0.525$.

Fig. 11 shows the effect of mixing with non-periodic stochastic spikes on SPs and the final number of links. For the non-periodic stochastic spikes we also use Poisson processes. The average firing rate of the mixed spikes that input to neurons are kept as 50Hz. For a spike train with mixing ratio of 50% (25%), we repeat a spike sequence that is truncated from a 25Hz (37.5Hz) Poisson spike train, and superimpose a 25Hz (12.5Hz) Poisson spike train. We find that the particular SP does not change in the case where we mix the periodic spike trains with non-periodic stochastic spikes. Because of the stochastic aspect of the spike trains, when a higher mixing ratio is used, fewer links survive.

## The influence of different parameters in STDP

Next, we analyze the influence of different parameters in STDP, such as the asymmetrt parameter $\alpha$, the maximum peak synaptic conductance $g_m$ and the synaptic delay $\tau_d$.

Figs. 12a and 13a show the influence of the asymmetry parameter $\alpha$ and the maximum peak synaptic conductance $g_m$ in STDP rule on the SPs of evolved networks respectively. From these figures, we find that the SPs do not change significantly under parameter variations (see also figs. 12b and 13b). We see that there are some dependencies between different motifs. For example, the forward cascade (triad 3) and the FFL (triad 7) are anti-correlated, while MFFL1 and MFFL2 (triad 9 and 10) as well as the anti-motifs triads 1 and 2 vary almost identically. As is seen from fig. 14, the synaptic delay likewise has little influence on the SP.
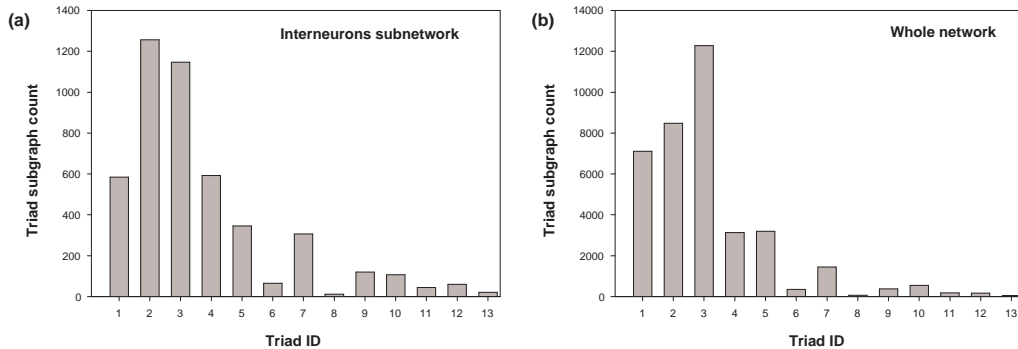
FIG. 2: Triad subgraph frequency spectrum of (a) the subnetwork of interneurons and (b) the whole network in *C. elegans*. The structure corresponding to each triad ID is shown in fig. 3.
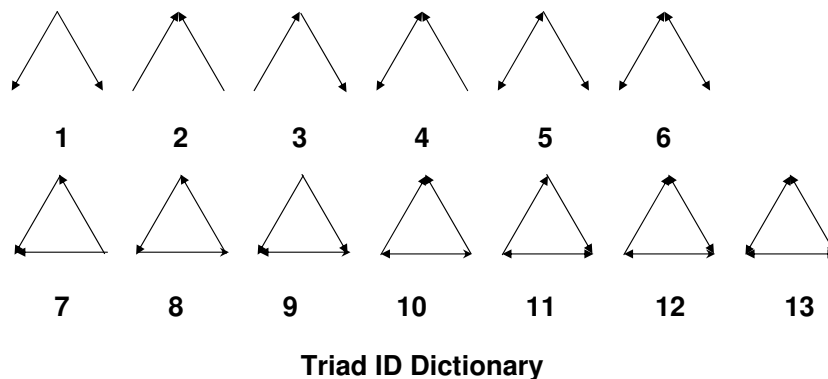


**Triad ID Dictionary**

FIG. 3: The network structure corresponding to each triad ID.

## DISCUSSION

We have studied the effect of the STDP learning rule on the network evolution systematically. The network is all-to-all connected initially. Neurons are stimulated with spike trains, which are (partially) periodic or temporally correlated in a more complicated way and in line with Poisson statistics. The STDP learning rule introduces the necessary competition between synapses. As the network evolves, a stationary distribution of peak synaptic conductances is achieved, where most synapses become weak enough to get pruned. In the STDP-driven evolved networks, three important triads FFL, MFFL1 and MFFL2, which are important for neural computation and cognition tasks, have been found with much higher frequency than expected from a randomized network. This implies that STDP could be a self-organization mechanism that generates these motifs.

The particular SP we found in STDP-driven evolved networks is quite robust against parameter variations. The characteristic of SP does not change essentially no matter what configurations are used, e.g. different neuron models, asymmetric or symmetric time windows, different asymmetric ratios $\alpha$, different maximum peak synaptic conductances $g_m$, different network sizes, different synaptic delays, different lengths of input sequences, and mixtures with non-periodic Poisson spike trains. This suggests that we have found a fundamental characteristic of STDP.

Our simulations mimic the biological case wherein the brain is densely wired at the time of birth and then most synapses are pruned in the course of development. To inspect whether STDP may play a role in the real case, we have compared our simulation results with the *C. elegans* neuronal system. We have investigated the most recently published wiring diagram of *C. elegans*, and analyzed the SPs of different subnetworks in the *C. elegans* neuronal systems. The SPs of STDP-driven evolved networks are quite similar to those in the *C. elegans* neuronal network, especially the subnetwork of interneurons. Besides, the triad frequency spectrum of STDP-driven evolved network in certain configurations is similar to that of *C. elegans*. The exact role of input in deciding the network structure is not
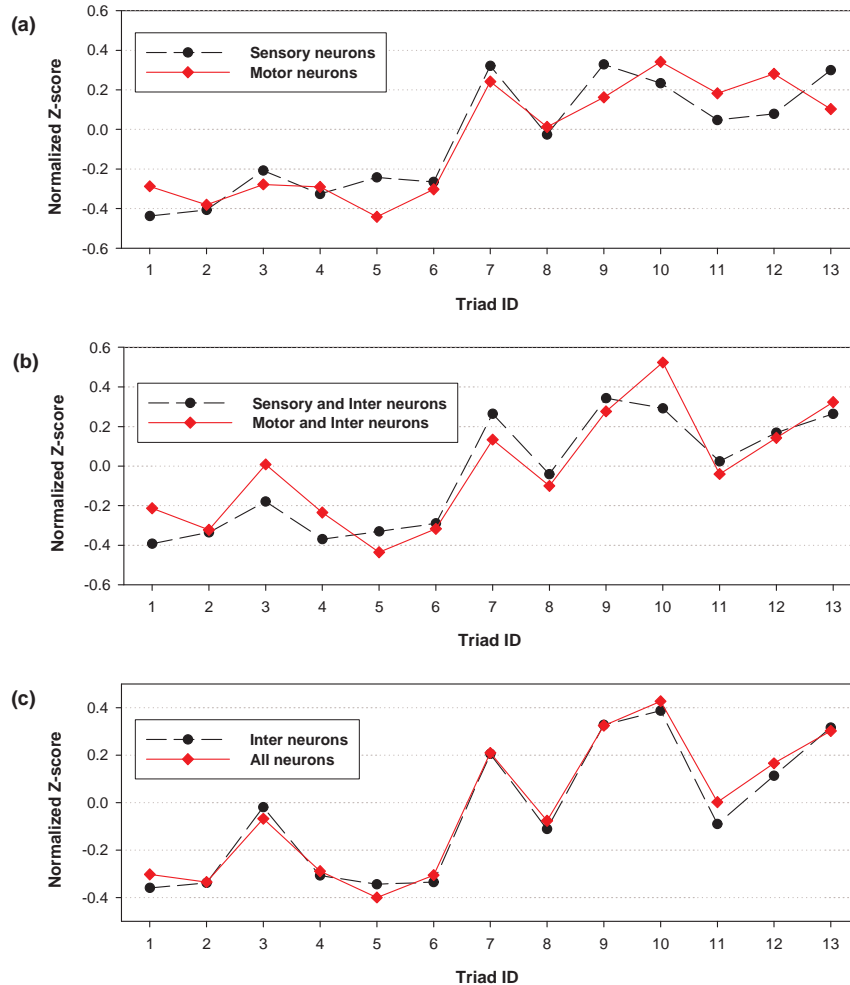
FIG. 4: (color online) The triad significance profile of different subnetworks in the *C. elegans* neuronal system. The lines connecting the Z-score values have been added only as a visualization aid. The structure corresponding to each triad ID is shown in fig. 3.

yet clear but it seems that some amount of complexity is needed. The sparsity of the *C. elegans* neuronal network could be also achieved by the STDP-driven evolved network. These observations show that the STDP self-organization mechanism could be a candidate to generate the local structure of *C. elegans* neuronal network.

In this study, we only consider STDP synapses and neglect other mechanisms such as short-term plasticity and gap connections that are present in *C. elegans*. Moreover, the neuron models and parameter setting may also be different from *C. elegans*. These factors all could influence the results. For example, gap connections are bi-directional in *C. elegans*, and could influence the dynamics of neurons. As the STDP learning rule depends on spiking activity, the existence of gap connections could influence the structure of an STDP-driven evolved network. The few observed differences between the simulated networks and the *C. elegans* neuronal network may be due to one of these reasons. In any case, the similarities between the two networks are striking considering the fact that such other complications have not yet been included.

The method of motif analysis we used is based on the algorithm of Milo *et al.* [22], which is widely used in different scenarios. Randomization is performed by rewiring connections. It features include: It keeps the number of incoming edges, outgoing edges and mutual edges of each node fixed. Motifs are counted here on the basis of the number of vertices they involve. So, for instance, triad 1 is a motif at the same level as, for instance, 7 because they both involve 3 vertices. In particular, 1 is not counted as a submotif of 7 because 7 contains an edge that is absent in 1. Conceptually, a problem with this approach is that such motif counts are not statistically independent. In particular, keeping the counts for certain triads fixed may not be a good null model in statistical terms. A more principled
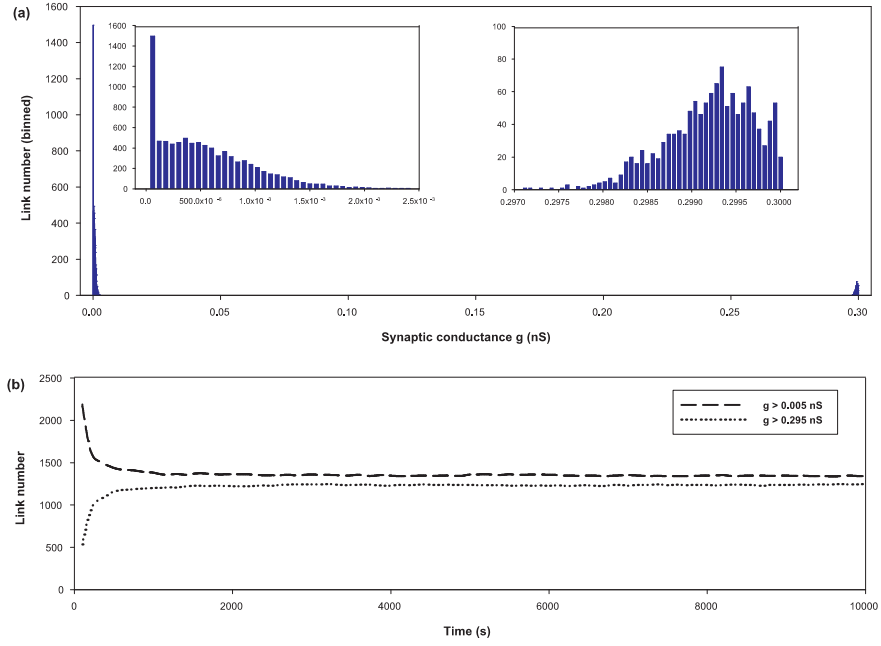
FIG. 5: (color online) (a) The final distribution of peak synaptic conductances $g$. (b) The variation of the link numbers of synapses whose peak conductance $g$ is above 0.005nS or 0.295nS. The parameter values are the same as in the "basic configuration" described in text.
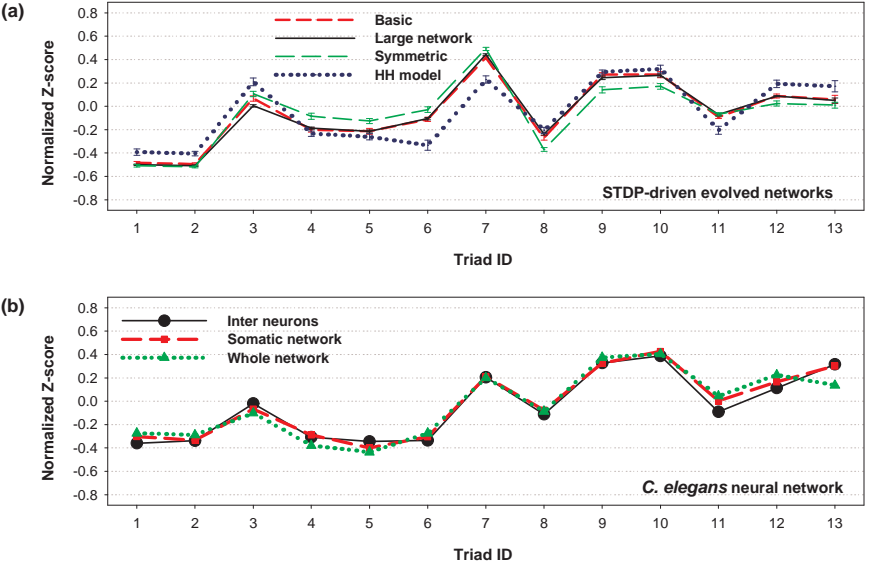


FIG. 6: (color online) Comparison of SPs for STDP-driven evolved networks and *C. elegans* neuronal network. (a) The SPs of four different STDP-driven evolved networks with different configurations: (i) Basic configuration; (ii) Symmetric configuration; (iii) HH model configuration; (iv) Large network configuration. (b) The SPs of *C. elegans* neuronal systems: (i) the subnetwork of somatic interneurons, (ii) the somatic network, (iii) the whole neuronal network of the old wiring diagram in [12]. The structure corresponding to each triad ID is shown in fig. 3.
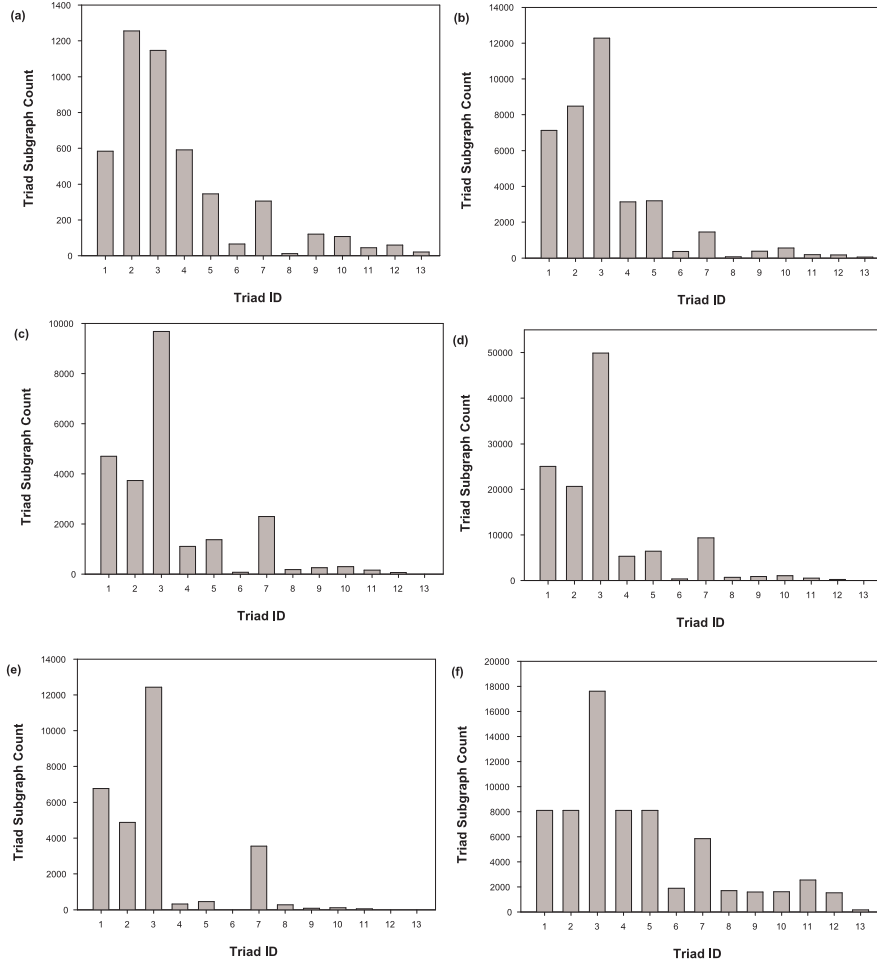
FIG. 7: Comparison of triad frequency spectra for STDP-driven evolved networks and *C. elegans* neuronal network: (a) subnetwork of somatic interneurons in *C. elegans*, (b) somatic neuronal network in *C. elegans*, and STDP-driven evolved networks of (c) "basic configurations", (d) "large network configurations", (e) "symmetric configurations", and (f) "HH model configurations". The structure corresponding to each triad ID is shown in fig. 3.

approach is developed in [25, 26], based on correlations between edges, in such a manner that the motifs are arranged in terms of the number of edges they contain, as opposed to the number of vertices involved. We cannot go into the details, but the underlying rationale is that a network is characterized by the specific presence or absence of edges for some fixed set of vertices, and null models therefore should be given in terms of correlations up to some given number of edges. This, however, means that for instance, triad 1 becomes a submotif of 7 so that each occurrence of 7 also counts as an occurrence of 1. So far, however, that approach has been developed only for undirected graphs. In any case, when we base the comparison of SPs between our STDP-driven evolved artificial network and the *C. elegans* neuronal network on that method, the similarities become much weaker. This may come about because by double counting, the SP of triads will be perturbed if there are variations in the SPs of more complex triads. These triads may be independent functional units when we start with a fully connected network and prune synapses according to the STDP learning rule, as opposed to beginning with a completely unconnected set of vertices and incrementally adding edges. It needs future work to explore this issue further.

The study suggests that the structure of a neuronal network is mostly determined by a correlation based learning mechanism. In particular, this seems to be based on self-organization on the basis of a local rule as opposed to a hard wired network scenario. The dynamical steady state reached also depends on the nature of the input supplied to neurons. This work identifies the important factors that determine the structure of the network. The conclusions might be useful in the choice of the neuronal substrate in large scale neural network simulations of the brain.
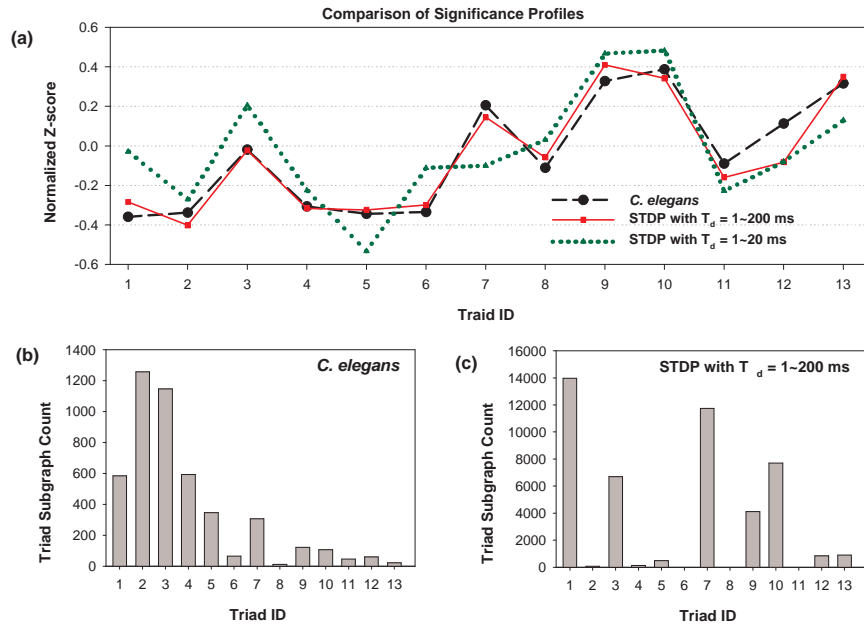
FIG. 8: (color online) Comparison of SPs and triad frequency spectra for the *C. elegans* interneuron subnetwork and STDP-driven evolved networks with correlated stochastic inputs. The structure corresponding to each triad ID is shown in fig. 3.
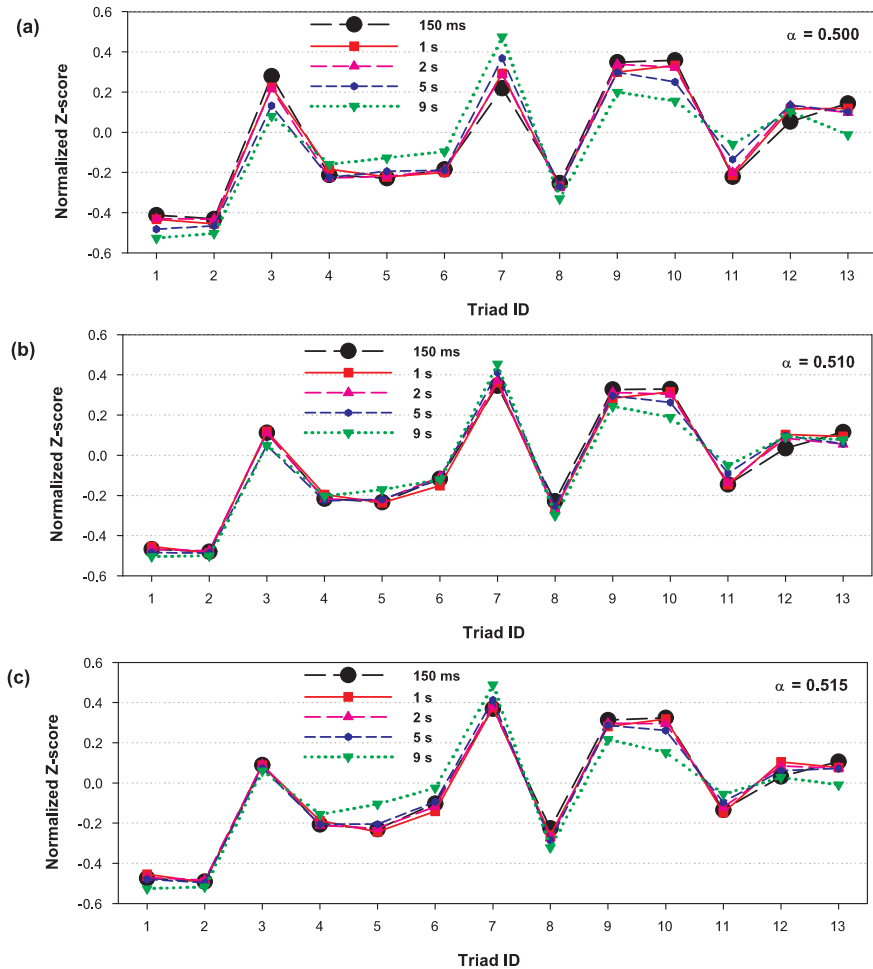


FIG. 9: (color online) The effect of input spike sequence period $T_{pattern}$ on SPs of STDP-driven evolved networks with different asymmetric parameter $\alpha$ of STDP rule: (a) $\alpha = 0.500$, (b) $\alpha = 0.510$, (c) $\alpha = 0.515$. Different periods $T_{pattern}$ studied are: 150ms, 1s, 2s, 5s and 9s. The structure corresponding to each triad ID is shown in fig. 3.

$^{*}$ Electronic address: `jost@mis.mpg.de`
[1] R. Albert, A.-L. Barabsi, Statistical mechanics of networks, Rev. Mod. Phys. 74 (2002) 47–97.
[2] D. Watts, S. Strogatz, Collective dynamics of small-world networks, Nature 393 (1998) 440–442.
[3] S. Bornholdt, H. G. Schuster, Handbook of Graphs and Networks: From the Genome to the Internet, Wiley-VCH, Weinheim, 2002.
[4] M. E. J. Newman, The structure and function of complex networks, SIAM Review 45 (2003) 167–256.
[5] S. N. Dorogovtsev, J. F. F. Mendes, Evolution of Networks: From Biological Nets to the Internet and WWW, Oxford University Press, USA, 2003.
[6] V. M. Eguíluz, D. R. Chialvo, G. A. Cecchi, M. Baliki, A. V. Apkarian, Scale-free brain functional networks, Phys. Rev. Lett. 94 (1) (2005) 018102. `\path{doi:10.1103/PhysRevLett.94.018102}`.
[7] C. J. Stam, J. C. Reijneveld, Graph theoretical analysis of complex networks in the brain, Nonlinear Biomedical Physics 1 (2007) 3.
[8] H. Markram, J. Lübke, M. Frotscher, B. Sakmann, Regulation of synaptic efficacy by coincidence of synaptic APs and EPSPs, Science 275 (1997) 213–215.
[9] J. Jost, Temporal correlation based learning in neuron models, Theory Bioscienc. 125 (2006) 37–53.
[10] J. Jost, K. M. Kolwankar, Evolution of network structure by temporal learning, Physica A 388 (2009) 1959.
[11] C.-W. Shin, S. Kim, Self-organized criticality and scale-free properties in emergent func tional neural networks, Phys. Rev. E 74 (2006) 045101(R).
[12] J. G. White, E. Southgate, J. N. Thomson, S. Brenner, The structure of the nervous system of the nematode caenorhabditis
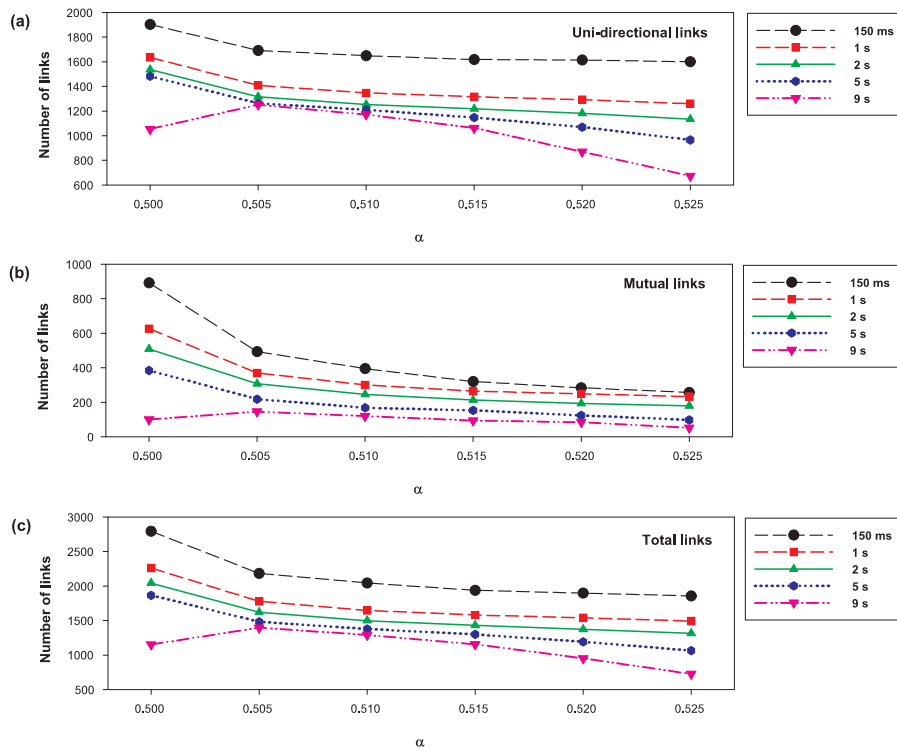
FIG. 10: (color online) The number of surviving links in networks with input spike trains of different periods: 150ms, 1s, 2s, 5s and 9s. Other parameters are as in the "basic configuration".
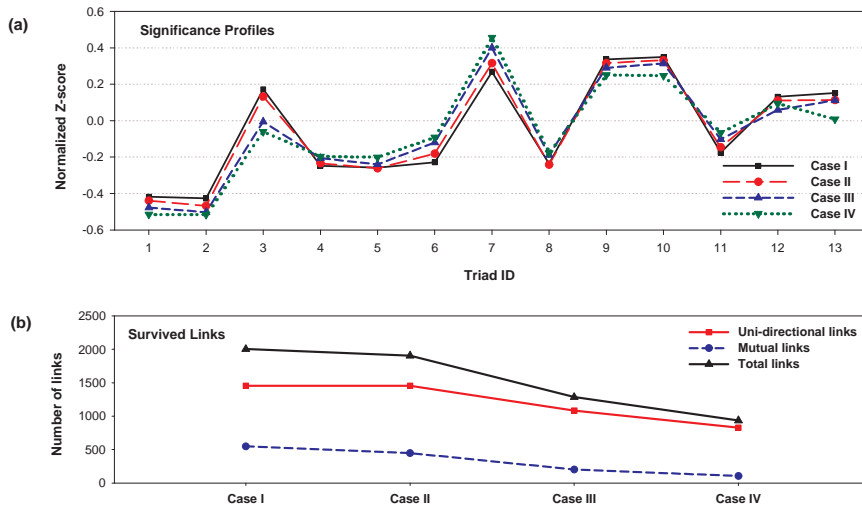


FIG. 11: (color online) The SPs and the number of surviving links in networks, which receive input of spike trains mixed with non-periodic Poisson spikes of different average firing rates: Case I, 13Hz stochastic Poisson processes & 37Hz periodic patterns with $\alpha = 0.5$; Case II, 25Hz stochastic Poisson processes and 25Hz periodic patterns with $\alpha = 0.5$; Case III, 13Hz stochastic Poisson processes & 37Hz periodic patterns with $\alpha = 0.55$; and Case IV, 25Hz stochastic Poisson processes & 25Hz periodic patterns with $\alpha = 0.55$. The period of the input patterns is set to 150ms to save simulation time, while other parameters are the same as in the "basic configuration". The structure corresponding to each triad ID is shown in fig. 3.
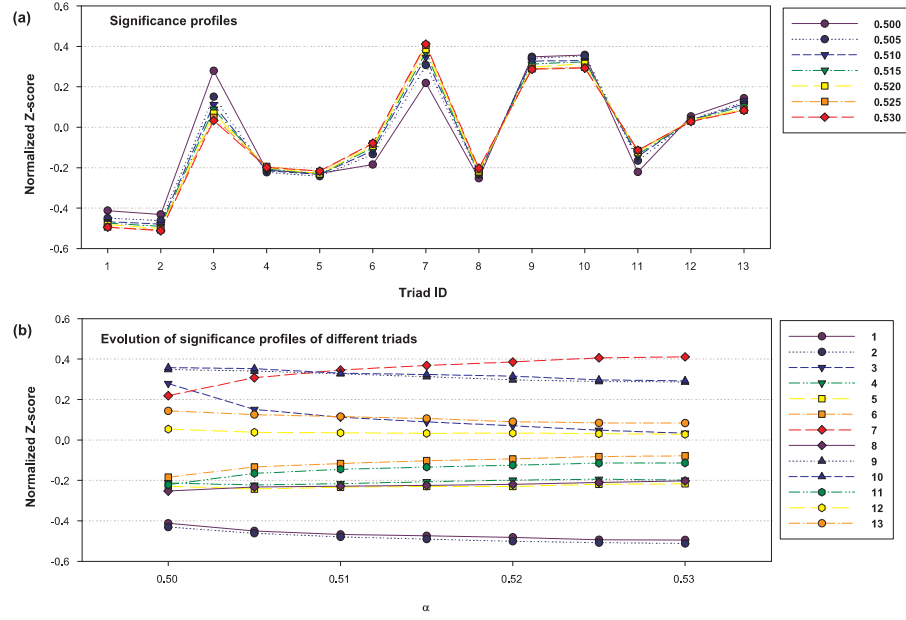
FIG. 12: (color online) The influence of the asymmetry parameter $\alpha$ in STDP rule on the SPs of evolved networks. (a) The SPs of networks with different $\alpha$. (b) The evolution of each triad SP along with different $\alpha$. The period of input patterns is 150ms, while the other parameters are as in the "basic configuration". The structure corresponding to each triad ID is shown in fig. 3.
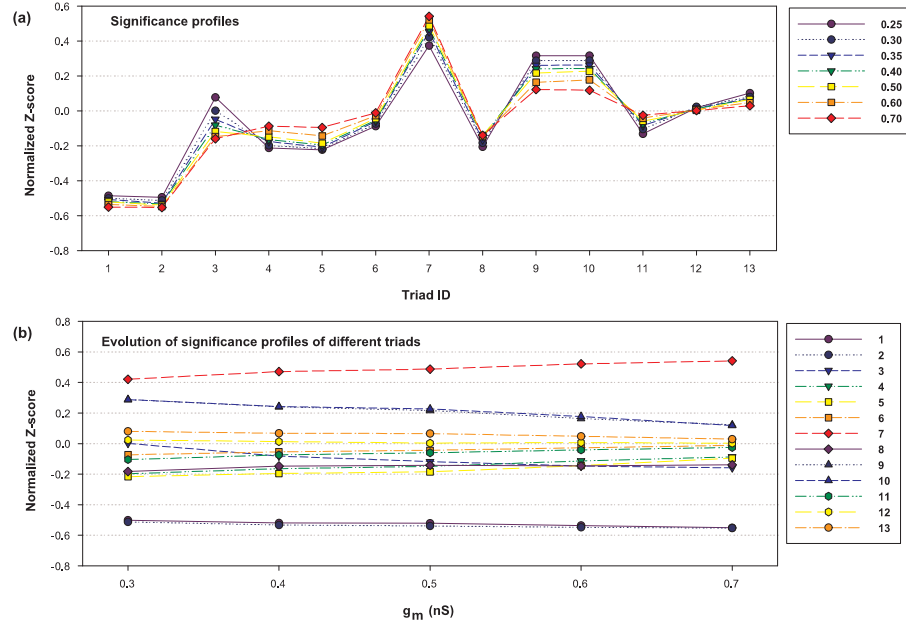


FIG. 13: (color online) The influence of the maximum peak synaptic conductance $g_m$ in STDP rule on the SPs of evolved networks. (a) The SPs of networks with different $g_m$. (b) The evolution of each triad SP along with different $g_m$. The period of input patterns is 150ms, while the remaining parameters are as in the "basic configuration". The structure corresponding to each triad ID is shown in fig. 3.
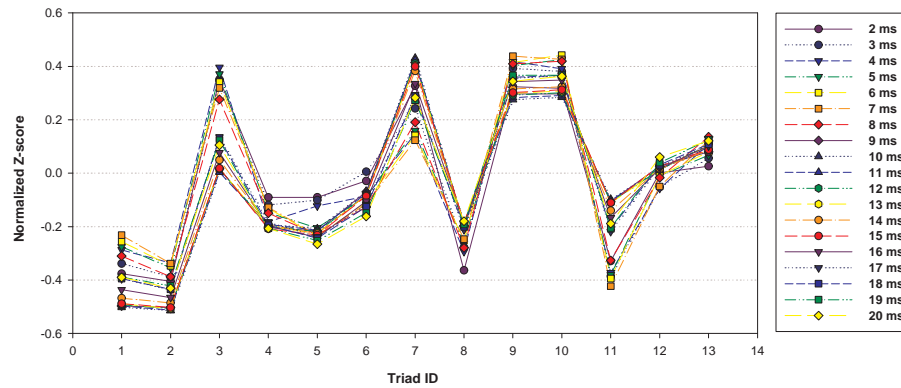
FIG. 14: (color online) The influence of synaptic time delay $\tau_d$ on the SPs of evolved networks. The period of input patterns is 150ms, $\alpha = 0.55$, while the other parameters are as in the "basic configuration". The structure corresponding to each triad ID is shown in fig. 3.

elegans, Phil. Trans. R. Soc. Lond. B 314 (1986) 1–340.

[13] L. R. Varshney, B. L. Chen, E. Paniagua, D. H. Hall, D. B. Chklovskii, Structural properties of the *Caenorhabditis elegans* neuronal networkSubmitted.

[14] D. L. Bishop, T. Misgeld, M. K. Walsh, W.-B. Gan, J. W. Lichtman, Axon branch removal at developing synapses by axosome shedding, Neuron 44 (4) (2004) 651 – 661. \path{doi:DOI:10.1016/j.neuron.2004.10.026}.

[15] W.Wadsworth, Axon pruning: C. elegans makes the cut, Current Biology 15 (2005) R796–R798.

[16] E. L. Peckol, J. A. Zallen, J. C. Yarrow, C. I. Bargmann, Sensoty activity affects sensory axon development in c. elegans, Development 126 (1999) 1891.

[17] M.-O. Gewaltig, M. Diesmann, Nest (neural simulation tool), Scholarpedia 2 (4) (2007) 1430.

[18] S. Song, K. D. Miller, L. F. Abbott, Competitive hebbian learning through spike-timing-dependent synaptic plasticity, Nature Neuroscience 3 (9) (2000) 919–926.

[19] R. D. Traub, R. Miles, Neuronal Networks of the Hippocampus, Cambridge University Press, Cambridge UK., 1991.

[20] N. Brunel, V. Hakim, Fast global oscillations in networks of integrate-and-fire neurons with low firing rates, Neural Computation 11 (1999) 1621–1671.

[21] R. Milo, S. Shen-Orr, S. ltzkovitz, N. Kashtan, D. Chklovskii, U. Alon, Network motifs: Simple building blocks of complex networks, Science 298 (2002) 824–827.

[22] R. Milo, S. Itzkovitz, N. Kashtan, R. Levitt, S. Shen-Orr, I. Ayzenshtat, M. Sheffer, U. Alon, Superfamilies of evolved and designed networks, Science 303 (2004) 1538–1542.

[23] U. A. etc. \path{arXiv:http://www.weizmann.ac.il/mcb/UriAlon/}.

[24] J. G. Foster, D. V. Foster, P. Grassberger, M. Paczuski, Link and subgraph likelihoods in random undirected networks with fixed and partially fixed degree sequences, Phys. Rev. E 76 (2007) 046112.

[25] T. Kahle, E. Olbrich, J. Jost, N. Ay, Complexity measures from interaction structures, Phys. Rev. E 79 (2009) 026201.

[26] E. Olbrich, T. Kahle, N. Bertschinger, N. Ay, J. Jost, Quantifying structure in networks, Proc. ECCS 09.

[27] P. Kaluza, M. Ipsen, M. Vingron, A. S. Mikhailov, Design and statistical properties of robust functional networks: A model study of biological signal transduction, Phys. Rev. E 75 (2007) 015101(R).

[28] K. Klemm, S. Bornholdt, Topology of biological networks and reliability of information processing, PNAS 102 (2005) 18414–18419.

[29] P. R. Huttenlocher, Synaptic density in human frontal cortex - developmental changes and effects of aging, Brain Res. 163 (1979) 195–205.

[30] G. Q. Bi, M. M. Poo, Synaptic modification by correlated activity: Hebb's postulate revisited, Annu. Rev. Neurosci. 24 (2001) 139–166.

[31] C. Li, Functions of neuronal network motifs, Phys. Rev. E 78 (2008) 037101.

[32] N. Masuda, H. Kori, Formation of feedforward networks and frequency synchrony by spike-timing-dependent plasticity, J. Comput. Neurosci. 22 (2007) 327–345.

[33] Y. K. Takahashi, H. Kori, N. Masuda, Self-organization of feed-forward structure and entrainment in excitatory neural networks with spike-timing-dependent plasticity, Phys. Rev. E 79 (2009) 051904.

[34] T. Nowotny, M. I. Rabinovich, Spatial representation of temporal information through spike-timing-dependent-plasticity, Phys. Rev. E 68 (2003) 011908.